SCIENCE CHINA
Physics, Mechanics & Astronomy

• Article •
Special Issue: Physical Mechanics

June 2012 Vol.55 No.6: 1093–1097
doi: 10.1007/s11433-012-4758-x

Crack and size-dependence of shear modulus in a drying particulate film

CAO He[1,2], LAN Ding[1] & WANG YuRen[1*]

[1] *Key Laboratory of Microgravity (National Microgravity Laboratory), Institute of Mechanics, Chinese Academy of Sciences, Beijing 100190, China;*
[2] *Institute of Microelectronics, Chinese Academy of Sciences, Beijing 100029, China*

Received February 16, 2012; accepted April 17, 2012; published online April 27, 2012

We utilized controlled vertical drying deposition (CVDD) method, which can fabricate a uniform face-center-cubic (FCC) structure film, to investigate the crack formation and the size dependence of shear modulus in a drying particulate film. We found that both crack spacing and shear modulus depend on colloidal particle size. They drop with increase of particle radius (R) in a single range. Furthermore, compared with the shear modulus variation of a dry particulate film, it was found that both solid part and liquid part in a drying particulate film play equivalent roles in the film mechanical behavior.

crack formation, size dependence, shear modulus, colloidal film

PACS number(s): 42.70.Qs, 83.80.Hj, 62.20.Mk, 81.40.Np

Citation: Cao H, Lan D, Wang Y R. Crack and size-dependence of shear modulus in a drying particulate film. Sci China-Phys Mech Astron, 2012, 55: 1093–1097, doi: 10.1007/s11433-012-4758-x

1 Introduction

When a layer of fluid containing submicron sized colloidal particles is dried on a nonporous rigid substrate, a close packed array is formed following the evaporation of the solvent. It is currently observed in many applications, such as ink jet paper, paints, ceramic films, photographic films and colloidal crystals. However, cracks will appear and inevitably degenerate the film integrity because of the existence of enormous stresses stemming from the drying process. Cracks were found to align in parallel to the drying direction at the initial crack formation stage and form a periodic crack pattern with a single wavelength for many drying systems [1–4]. The mechanism for the crack formation was also discussed in the literature [5–7]. The cracking mechanism is widely accepted to be a result of capillary pressure, developed in the particulate networks as solvent evaporates. Two kinds of experiments are usually employed in these studies. One is the droplet-like drying method [3–6,8], while the other is the directional drying method [4,7,9]. Fracture mechanics was widely used to explain the thickness-dependence of crack spacing [5,10]. However, the effects of microstructures, such as particle radius, are rarely investigated.

It is well known that crack formation, in most cases, is strongly related to modulus of the material studied. However, the direct measurement for the shear modulus of a drying film is almost not possible and it is difficult to clarify the role of shear modulus in the drying process and crack formation by utilizing the above two experimental systems. The difficulties come from the fact that the drying process undergoes a gelation process and subsequently forms a structure largely deviated from an ideal crystalline structure. Furthermore, the stress status and its evolution were complex in the whole drying process. To further understand the mechanical properties of drying particulate film, a simple

*Corresponding author (email: yurenwang@imech.ac.cn)

drying system is needed which should possess the following two priorities; firstly, the gelation process should be excluded in the whole drying process and secondly, a more uniformly ordered structure needs to be obtained, which can then simplify the calculation of stress, deformation energy or any other related physical quantities.

In this work, the CVDD method was employed to produce the reputed simple drying system. The CVDD method uses a drying system that is reported to make high-quality single crystal films [11,12], which is formed of colloidal particles on glass substrates coming from a low concentration water suspension (such as 0.1% volume fraction). The self-assembly of colloidal particles is controlled by capillary force and internal flow in the vicinity of meniscus during the whole film formation process [13–15]. Colloidal particles are randomly captured and form a single crystal colloidal film with a specific crystal structure, such as FCC structure. During the whole drying process, the water suspension was kept at a low concentration. Therefore, the gelation process is avoided. It strongly simplifies the variation of stress state during the drying process. Also, the crystal structure of the drying film fabricated by the CVDD gives us an opportunity to analyze the crack formation of drying film by atomic crystal fracture theory.

We studied the size-dependence of shear modulus of the drying film and found that it is strongly dependent on the particle radius. It dropped as the particle radius increased in a single range. Moreover, comparing our results with the variation of the shear modulus of dry particulate film [16–18], we found that not only the solid structure of colloidal particles but also the infiltration water plays a decisive factor in determining the mechanical behavior of drying particulate films.

2 Experimental

Figure 1 shows the schematic diagram of the experimental setup for *in situ* observation of evaporation-induced self-assembly [19–21]. To have a comprehensive understanding of the assembly process of CVDD, a magnified schematic of the observed region was shown, as well as the image observed at the initial growth stage. Large colloid spheres with the diameter of 3 μm were used for the observation of the initial assembly process. Initial fracture for the film with 110 nm particle radius is shown at the bottom-right corner. We observed the drying aqueous suspensions in a transparent cell at the controlled constant temperature 50°C. Polystyrene spheres (from Duke Scientific Corporation, USA) with diameters of 170, 220, 300, 360 and 430 nm were used in the experiments. Polystyrene spheres were mono-dispersed in super-pure water with 0.1% volume fraction. The suspension was transferred into a semi-cylindrical glass growth cell. A 4 mm×1.2 mm rectangular glass substrate was inserted vertically into the growth cell. To guarantee

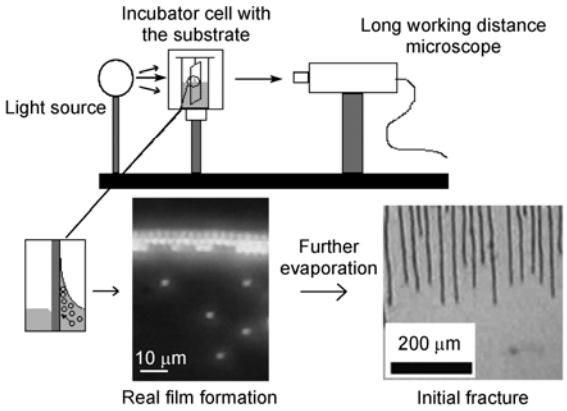

Figure 1 Schematic diagram of the experimental setup. A magnified schematic of the observed region is shown in the vicinity of the meniscus, as well as the image observed at the initial growing stage. Large colloid spheres with the diameter of 3 micrometers were used. Also, initial fracture of the film with 110 nm particle radius is shown at the bottom-right corner.

good hydrophilicity of the substrate, the glass substrate and the growth cell walls were cleaned with detergent, followed by immersion in chromic acid for about 24 h. Cleaned glass plates were kept in super-pure water and dried naturally before the experiment. Glass growth cell was kept at 50°C during the experiment to control evaporation rate. The mean evaporation rate was about 0.17 g/h and films formed with nearly the same thicknesses ($h \approx 6.3$ μm). A long working distance optical microscope was used to carry out experiments. The observation was focused on the initial cracks evolution in the vicinity of the suspension meniscus. The experimental data was recorded with a digital video recorder.

3 Results and discussion

3.1 The size-dependence of crack spacing

From *in-situ* observations of the initial crack formation during the drying of the colloidal film, it can be seen that parallelly straight cracks covered the full screen. The cracks grew to the drying front and invaded the whole sample as evaporation continued. The thickness of dried films was about 3.6 μm, measured by scanning electron microscope (SEM). Figure 2 shows a plot of the crack spacing against the particle radius. It can be seen that the crack spacing increased as particle radius decreased. This phenomenon was not reported in droplet-like drying systems and the directional drying systems. As we mentioned above, gelation is an inevitable process and the structures of their films formed by these drying systems are not uniform. Therefore, the comparability among the crack behaviors of drying films with diverse particle sizes was greatly reduced. Thus the relationship between crack spacing and particle size were not revealed in these drying systems. In our experi-

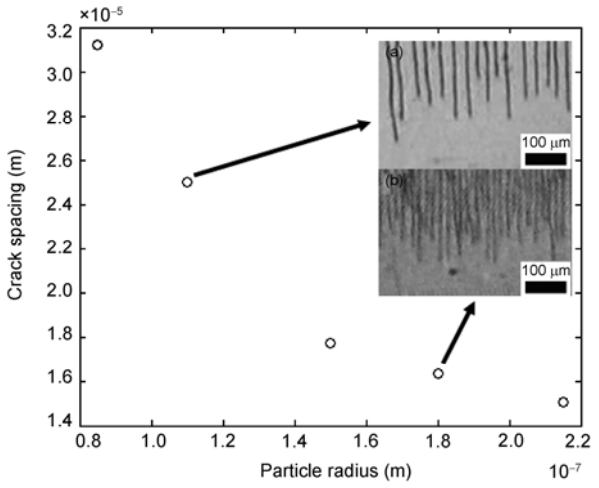

Figure 2 Crack spacings observed for the drying films with different particle sizes. (a) and (b) are the observing pictures for the films with R=110 nm and R=180 nm PS spheres, respectively.

ments, the CVDD method does not undergo a gelation process and can fabricate a uniform film with FCC structure. All films are of the same geometrical structure and in similar stress state. Thus, the real relationship between crack spacing and particle radius by observation is easily revealed in our observation, namely, crack spacing increased as particle radius decreased.

3.2 The size-dependence of shear modulus

It is well known that cracks are the external representation of the mechanical properties of a material. Tirumkudulu and Russel [5] utilized energy balance analysis to predict crack dynamics for multiple cracks. They found that the fracture stress of drying film (σ_1) was related to shear modulus (G), crack spacing ($2W$), film thickness (h), interfacial energy between water and air (γ_{wa}), solid volume fraction (Φ) and number of neighbor particles (M). The equation can be expressed as:

$$\sigma_1 = C_1 \cdot \frac{[G(R)]^{1/3}}{[f(W)]^{2/3}}, \tag{1}$$

where

$$C_1 = \left[\frac{4\gamma_{wa}\sqrt{\frac{3}{35}M\Phi}}{-3h\left(\frac{1}{\bar{k}} - \frac{\bar{k}}{3}\right)} \right]^{\frac{2}{3}},$$

$$f(W) = \tanh\left(\frac{\bar{k}W}{2h}\right) - \frac{1-\bar{k}^2}{3-\bar{k}^2} \cdot \frac{\bar{k}W/2h}{\cosh^2\left(\bar{k}W/2h\right)}$$

and $\bar{k}$ is given as a constant.

In our case, the colloidal particles in the drying film formed a uniform FCC structure, thus, h, γ_{wa}, Φ and M in eq. (1) are constants. Thus, one of shear modulus and fracture stress, or both, must be related to particle radius. It is reasonable to suppose shear modulus is a function of particle radius, namely, is G=$G(R)$. This took the problem that both shear modulus and fracture stress are unknown quantities and we cannot elucidate them from only one equation. Fortunately, CVDD was specialized in making high-quality single crystal films (Figure 3). The geometrical structure and the interactions among colloidal particles are analogous to atomic crystal structure. Thus, we can calculate the theoretical critical stress of drying film by atomic crystal fracture theory.

In our previous work [22], we considered van der Waals attraction as the key factor that determines the interfacial energy between two solid surfaces and assumed the film cracks along the $(1\bar{1}0)$ crystallographic planes. The critical stress for crack propagation was given as:

$$\sigma_0 = \frac{\sqrt{2}A}{96Z_0^2}\left(\frac{1}{R} + \frac{0.191}{Z_0}\right), \tag{2}$$

where Z_0 is the minimum distance between the particles and A is the Hamaker constant.

The actual stress is always smaller than the theoretical value because of the presence of lattice defects and micro-cracks between particles, which can significantly decrease the structural strength of the colloidal crystal. It is reasonable to assume that the actual colloid crystal fracture stress is several times less than the theoretical strength. Here, we take eq. (1) as the actual stress, and compared it with eq. (2). If we take R=110 nm as the reference, we can derive

$$\sigma(R) = \frac{\sigma_1(R=110\text{ nm})}{\sigma_0(R=110\text{ nm})}\sigma_0(R) \tag{3}$$

as the real critical stress.

Substitution of eq. (3) into eq. (1) yields

$$\frac{G(R)}{G(R=110\text{ nm})} = \left\{\frac{f(W)}{f(W_{R=110\text{ nm}})}\right\}^2 \times \left\{\frac{\sigma_0(R)}{\sigma_0(R=110\text{ nm})}\right\}^3. \tag{4}$$

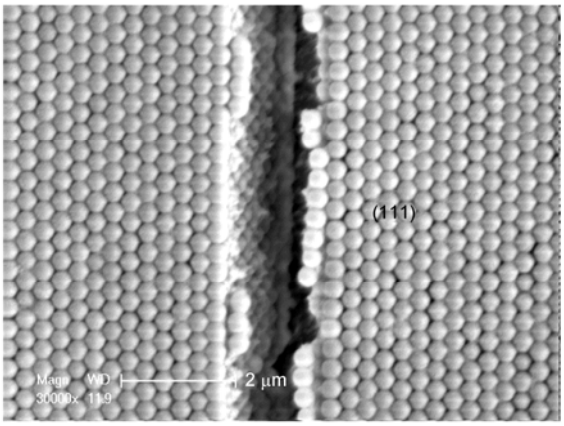

Figure 3 SEM image for the film formed by CVDD.

In order to make eq. (4) dimensionless, we take $\overline{G} = G(R)/G(R=110\text{ nm})$ and $\overline{R} = R/R_0$, where R_0 is 150 nm. Constants Z_0, A, M, Φ_{rcp}, $\overline{k}$, and γ_{wa} are listed in Table 1. Substituting these parameters into eq. (4), we get a nondimensionalized equation:

$$\overline{G} = 2.61\times10^{-6}\times\left\{\frac{f(W)}{f(W_{R=110\text{ nm}})}\right\}^2\times\left(\frac{1}{\overline{R}}+71.625\right)^3. \quad (5)$$

From eq. (5) and the experimental data shown in Figure 2, we can get the values of the nondimensionalized shear modulus for different nondimensionalized particle radius (Table 2). It can be seen that nondimensionalized shear modulus of colloidal crystal structures during drying process depends on the particle radius. It decreases as particle radius increases in a single range ($0.567 \leqslant \overline{R} \leqslant 1.667$). Furthermore, the shear modulus of the film with 110 nm particle radius, $G(R$=110 nm), is an unknown constant. Thus the shear modulus of drying films should show the same variation rule.

Furthermore, there are many similarities between dried particulate agglomerates and the solid structures of drying films. Firstly, particles form a certain structure arrangement, (for example, FCC) and secondly, the interactions among particles are almost the same. The study of mechanical properties of dried particular agglomerates is relatively mature and various theories about the Young's modulus have been reported [16–18]. For dried particulate agglomerates, particularly porous binderless granules, Kendall et al. [16], Thornton [17], Adams et al. [18] predicted the Young's modulus (E^*) of a particulate packing separately. The Young's modulus is proportional to 1/3-power of solid surface energy (Γ) and reciprocal proportion to 1/3-power of particle radius, which can be expressed as $E^* \propto (\Gamma/R)^{1/3}$.

In our case, because the surface energies of the solids are determined by Van der Waals attractive energy, Γ would be almost a constant for different particle radius. If we consider the Poisson's ratios of the films with different particle radius are the same and their shear modulus (G^*) should be proportional to their Young's modulus $G^* \propto E^*$. The nondimensionalized shear modulus can be given as:

$$\overline{G^*} = 0.578\times\left(\frac{1}{\overline{R}}\right)^{1/3}. \quad (6)$$

From Figure 4, it is evident that $\overline{G^*}$ drops as particle radius increases. This is not a surprising result, because a drying particulate film can be considered as a composite material composed of colloidal particles and fluid. The interactions among colloidal particles are similar with dried ones. When cracks appear, the solid part of drying film is broken down as in dried particulate agglomerates. Although it has never been documented before, the importance of solid structures in drying film has been realized. They enhanced the film strength by increasing the surface energies of the solid parts to form a crack-free film [27]. However, there is a seeming divergence between these two results while particle radius is reduced. The existence of liquid phase influences the mechanical properties of drying films. This effect increases when particle radius decreases. It may be due to the interactions between solid part and liquid part, such as friction drag. Friction drag is found in the viscous shear force of liquid or gas. The viscous force magnitude is inversely proportional to the square of characteristic dimension, which is particle radius R in this case. Thus, when the particle radius decreases, the viscous force will increase. There is a bigger divergence between our theory and the prediction for dried particulate agglomerates in refs. [16–18] when particle radius decreases.

Table 1 Experimental constants used in theoretical analysis

A (J) [a]	M [b]	Z_0 (nm) [c]	Φ	γ_{wa} (N/m)	$\overline{h}$ (m)	$\overline{k}$ [d]
1.0×10^{-20}	6	0.4×10^{-9}	0.74	0.073	6.3×10^{-6}	0.699

a) Ref. [23]
b) Ref. [24]
c) Ref. [25]
d) Ref. [26]

Table 2 Nondimensionalized shear modulus of different nondimensionalized particle radius

$\overline{R}$	$\overline{G}$
0.57	1.469
0.73	1.015
1.00	0.546
1.20	0.465
1.43	0.396

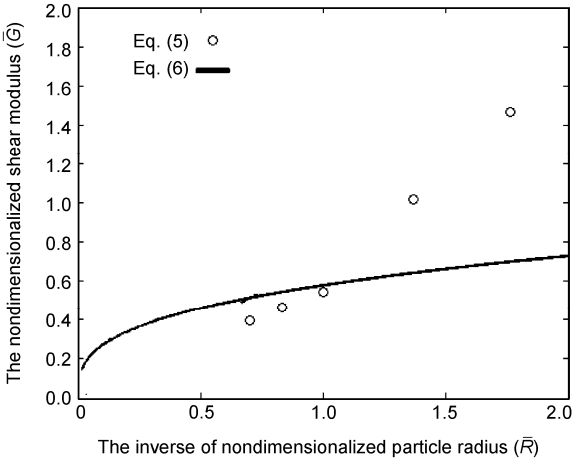

Figure 4 Relationship between $\overline{G}$ and $1/\overline{R}$ revealed in our experiments compared with the prediction from refs. [16–18] for dried particulate agglomerates.

4 Conclusion

We have utilized the CVDD method, which can fabricate a uniform FCC structure film, to simplify drying process. We focused on the size dependence of crack spacing and shear modulus of a drying film. We found that both crack spacing and shear modulus depend on colloidal particle size. They drop with increase of particle radius (R) in a single range. Furthermore, we compared our results with the variation of the shear modulus of the dry particulate film to investigate the source mechanical properties of drying film. We found that not only the solid structure but also the liquid part is a decisive factor to determine the mechanical behaviors of drying particulate films. The interactions between solid part and liquid part, such as friction drag, may have an important role when the particle radius decreases.

This work was supported by the National Basic Research Program of China (Grant No. 2011CB710901) and the Knowledge Innovation Program of the Chinese Academy of Sciences (Grant No. KJCX2-YW-L08).

1 Skjeltorp A T, Meakin P. Fracture in microsphere monolayers studied by experiment and computer simulation. Nature, 1988, 335: 424–426
2 Allain C, Limat L. Regular patterns of cracks formed by directional drying of a colloidal suspension. Phys Rev Lett, 1995, 74: 2981–2984
3 Pauchard L, Parisse F, Allain C. Influence of salt content on crack patterns formed through colloidal suspension desiccation. Phys Rev E, 1999, 59: 3737–3740
4 Shorlin K A, de Bruyn J R, Grahan M, et al. Development and geometry of isotropic and directional shrinkage-crack patterns. Phys Rev E, 2000, 61: 6950–6957
5 Tirumkululu M S, Russel W B. Cracking in drying latex films. Langmuir, 2005, 21: 4938–4948
6 Lee W P, Routh A F. Why do drying films crack? Langmuir, 2004, 20: 9885–9888
7 Dufresne E R, Corwin E I, Greenblatt N A, et al. Flow and fracture in drying nanoparticle suspensions. Phys Rev Lett, 2003, 91: 224501–224504
8 Chen K, Taflove A, Kim Y L, et al. Self-assembled patterns of nanospheres with symmetries from submicrons to centimeters. Appl Phys Lett, 2005, 86: 033101
9 Gauthier G, Lazarus V, Pauchard L. Alternating crack propagation during directional drying. Langmuir, 2007, 23: 4715–4718
10 Komatsu T, Sasa S. Pattern selection of cracks in directionally drying fracture: Part 1. Jpn J Appl Phys, 1997, 26: 391–395
11 Jiang P, Bertone J F, Hwang K S, et al. Single-crystal colloidal multilayers of controlled thickness. Chem Mater, 1999, 11(8): 2132–2140
12 Lan D, Wang Y R, Zhang Y M, et al. Small angle X-ray scattering of the colloidal crystal. Chin Phys C, 2009, 33(11): 1016–1018
13 Zheng Z, Gao K, Luo Y, et al. Rapidly infrared-assisted cooperatively self-assembled highly ordered multiscale porous materials. J Am Chem Soc, 2008, 130: 9785–9789
14 Denkov N D, Velev O D, Kralchevsky P A, et al. Interactions between particles with an undulated contact line at a fluid interface: Capillary multipoles of arbitrary order. Langmuir, 1992, 8: 3183–3190
15 Dimitrov A S, Nagayama K. Continuous convective assembling of fine particles into two-dimensional arrays on solid surfaces. Langmuir, 1996, 12: 1303–1311
16 Kendall K, Alford N M, Birchall J D. Elasticity of particle assemblies as a measure of the surface energy of solids. Proc R Soc A, 1987, 412: 269–283
17 Thornton C. On the relationship between the modulus of particulate media and the surface energy of the constituent particles. J Phys D-Appl Phys, 1993, 26: 1587–1592
18 Adams M J, McKeown R, Whall A. A micromechanical model for the confined uni-axial compression of an assembly of elastically deforming spherical particles. J Phys D-Appl Phys, 1997, 30: 912–920
19 Yang L, Zhang Y D, Luo J H, et al. Real-time studies of evaporation-induced colloidal self-assembly by optical microspectroscopy. Phys Rev E, 2011, 84 (3): 031605–031611
20 Yang L, Gao K Y, Luo Y H, et al. *In situ* observation and measurement of evaporation-induced self-assembly under controlled pressure and temperature. Langmuir, 2010, 27 (5): 1700–1706
21 Zheng Z Y, Liu X Z, Luo Y H, et al. Pressure controlled self- assembly of high quality three-dimensional colloidal photonic crystals. Appl Phys Lett, 2007, 90: 051910–051912
22 Cao H, Lan D, Wang Y R, et al. Fracture of colloidal single-crystal films fabricated by controlled vertical drying deposition. Phys Rev E, 2010, 82: 031602–031607
23 Israelachvili J. Intermolecular and Surface Forces, Amsterdam: Academic Press, 1991
24 Donev A, Cisse I, Sachs D, et al. Improving the density of jammed disordered packings using ellipsoids. Science, 2004, 303: 990–993
25 Krupp H. Particle adhesion theory and experiment. Adv Colloid Interface Sci, 1967, 1: 111–239
26 Routh A F, Russel W B. A process model for latex film formation: Limiting regimes for individual driving forces. Langmuir, 1999, 15: 7762–7773
27 Lee K, Asher S A. Photonic crystal chemical sensors: pH and ionic strength. J Am Chem Soc, 2000, 122: 9534–3537